Probing Fundamental Physics with Gravitational Waves

Cyril Lagger

THE UNIVERSITY OF SYDNEY

CoEPP
ARC Centre of Excellence for Particle Physics at the Terascale

Seminar - Universita di Bologna - February 18, 2018

Overwiev

Outline of this talk

The detection of Gravitational Waves (GWs) by LIGO/Virgo is promising for theoretical physics:

- confirms a prediction of General Relativity
- allows to test GR (and its extensions) in a strong and dynamical regime
- suggests to look for other sources of GWs in relation to particle physics: phase transitions, cosmic strings,...

Outline of this talk

The detection of Gravitational Waves (GWs) by LIGO/Virgo is promising for theoretical physics:

- confirms a prediction of General Relativity
- allows to test GR (and its extensions) in a strong and dynamical regime
- suggests to look for other sources of GWs in relation to particle physics: phase transitions, cosmic strings,...

This talk focuses on two topics:

- constraining noncommutative space-time from LIGO/Virgo waveforms (transient signal)
- exploring beyond the Standard Model physics with GWs from phase transitions (stochastic background)

Part I: Test of General Relativity and noncommutative space-time

First GW signal: GW150914

- Inspiral, merger and ring-down of a binary black hole observed by LIGO.
- Masses of $36^{+5}_{-4} M_\odot$ and $29^{+4}_{-4} M_\odot$.
- Frequency ranging from 35 to 250 Hz and velocity up to $\sim 0.5c$.

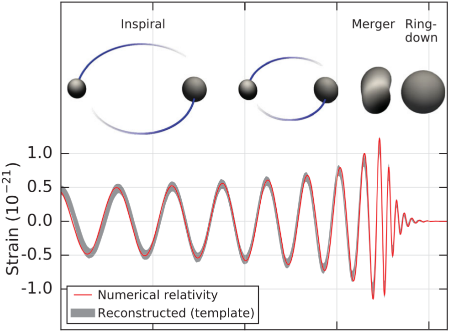

[LIGO/Virgo Coll., Phys. Rev. Lett. 116 (2016) 061102]

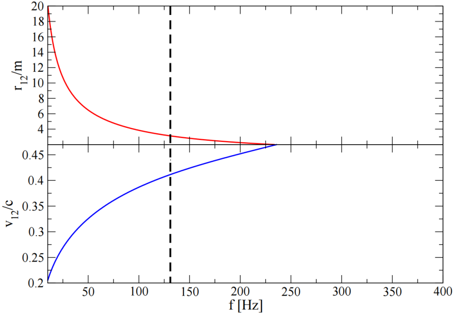

[N. Yunes, K. Yagi, F. Pretorius, arXiv:1603.08955]

An opportunity to test GR and its extensions

Einstein Field Equations (EFE) from General Relativity predicts the waveform of such GWs :

- post-Newtonian formalism provides an analytical expansion in $\frac{v}{c}$ (valid only during the inspiralling)
- numerical Relativity provides accurate simulations, including the merger and the ring-down

An opportunity to test GR and its extensions

Einstein Field Equations (EFE) from General Relativity predicts the waveform of such GWs :

- post-Newtonian formalism provides an analytical expansion in $\frac{v}{c}$ (valid only during the inspiralling)
- numerical Relativity provides accurate simulations, including the merger and the ring-down

GW150914 data are in good agreement with GR predictions

[LIGO/Virgo Coll., Phys. Rev. Lett. 116 (2016) 221101]

$\Rightarrow$ opportunity to test various models beyond GR.

[e.g.: N. Yunes, K. Yagi, F. Pretorius, arXiv:1603.08955, N. Yunes, E. Berti, K. Yagi, arXiv:1801.03208]

An opportunity to test GR and its extensions

Einstein Field Equations (EFE) from General Relativity predicts the waveform of such GWs :

- post-Newtonian formalism provides an analytical expansion in $\frac{v}{c}$ (valid only during the inspiralling)
- numerical Relativity provides accurate simulations, including the merger and the ring-down

GW150914 data are in good agreement with GR predictions

[LIGO/Virgo Coll., Phys. Rev. Lett. 116 (2016) 221101]

$\Rightarrow$ opportunity to test various models beyond GR.

[e.g.: N. Yunes, K. Yagi, F. Pretorius, arXiv:1603.08955, N. Yunes, E. Berti, K. Yagi, arXiv:1801.03208]

Our objective: constrain the scale of noncommutative space-time.

The post-Newtonian formalism

L. Blanchet, Living Rev. Rel. 17 (2014)

Definitions and notations

The full EFE in the harmonic gauge ($\partial_\mu h^{\alpha\mu} = 0$) can be written as

$$\Box h^{\alpha\beta} = \frac{16\pi G}{c^4} \tau^{\alpha\beta}$$

with the gravitational-field amplitude h and the matter-gravitational source τ:

$$h^{\alpha\beta} = \sqrt{-g} g^{\alpha\beta} - \eta^{\alpha\beta}, \qquad \tau^{\alpha\beta} = |g| T^{\alpha\beta} + \frac{c^4}{16\pi G} \Lambda^{\alpha\beta}.$$

Definitions and notations

The full EFE in the harmonic gauge ($\partial_\mu h^{\alpha\mu} = 0$) can be written as

$$\Box h^{\alpha\beta} = \frac{16\pi G}{c^4} \tau^{\alpha\beta}$$

with the gravitational-field amplitude h and the matter-gravitational source τ:

$$h^{\alpha\beta} = \sqrt{-g} g^{\alpha\beta} - \eta^{\alpha\beta}, \qquad \tau^{\alpha\beta} = |g| T^{\alpha\beta} + \frac{c^4}{16\pi G} \Lambda^{\alpha\beta}.$$

For a source term with characteristic velocity v, the post-Newtonian formalism (PN) solves the EFE as an expansion in powers of $\frac{v}{c}$. As a convention, a term of order n is called a $\frac{n}{2}$PN term and written as

$$\mathcal{O}(n) \equiv \mathcal{O}\left(\frac{v^n}{c^n}\right)$$

How to solve the full EFE?

Iterative expansions in the near and far zones and matching strategy in the overlap zone:

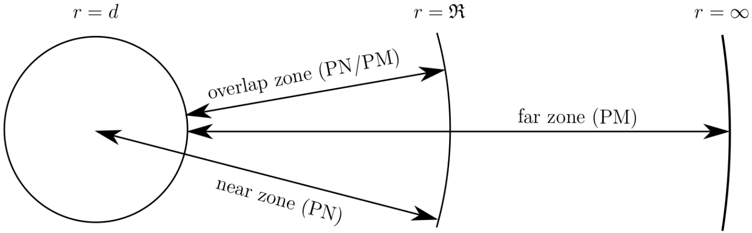

How to solve the full EFE?

Iterative expansions in the near and far zones and matching strategy in the overlap zone:

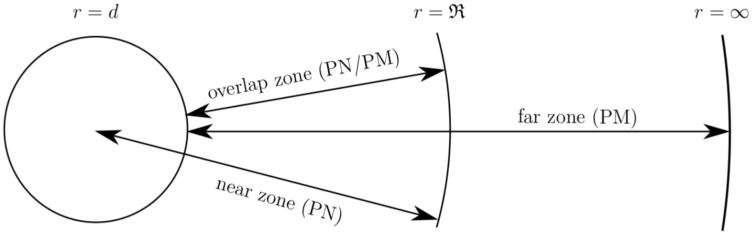

Post Minkowskian (PM) - G^n:

- $h^{\alpha\beta} = \sum_{n=1}^{\infty} G^n h_n^{\alpha\beta}$
- $\Box h^{\alpha\beta} = \Lambda^{\alpha\beta}$
- $\Box h_n^{\alpha\beta} = \Lambda_n^{\alpha\beta}[h_1, \cdots, h_{n-1}]$

How to solve the full EFE?

Iterative expansions in the near and far zones and matching strategy in the overlap zone:

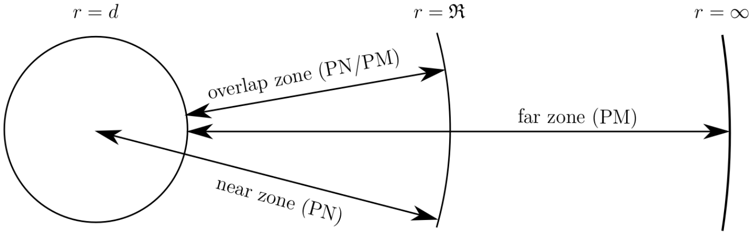

Post Newtonian (PN) - $\left(\frac{1}{c}\right)^n$:

- $h^{\alpha\beta} = \sum_{n=2}^{\infty} \frac{1}{c^n} h_n^{\alpha\beta}$
- $\tau^{\alpha\beta} = \sum_{n=-2}^{\infty} \frac{1}{c^n} \tau_n^{\alpha\beta}$
- $\nabla^2 h_n^{\alpha\beta} = 16\pi G\, \tau_{n-4}^{\alpha\beta} + \partial_t^2 h_{n-2}^{\alpha\beta}$

Post Minkowskian (PM) - G^n:

- $h^{\alpha\beta} = \sum_{n=1}^{\infty} G^n h_n^{\alpha\beta}$
- $\Box h^{\alpha\beta} = \Lambda^{\alpha\beta}$
- $\Box h_n^{\alpha\beta} = \Lambda_n^{\alpha\beta}[h_1, \cdots, h_{n-1}]$

Matter source

Consider a binary system of two black holes of masses m_1 and m_2. It is usually approximated by two point-like particles:

$$T^{\mu\nu}(\mathbf{x},t) = \frac{m_1}{\sqrt{g g_{\rho\sigma} \frac{v_1^\rho v_1^\sigma}{c^2}}} \; v_1^\mu(t) v_1^\nu(t) \; \delta^3(\mathbf{x} - \mathbf{y}_1(t)) + 1 \leftrightarrow 2$$

Matter source

Consider a binary system of two black holes of masses m_1 and m_2. It is usually approximated by two point-like particles:

$$T^{\mu\nu}(\mathbf{x},t) = \frac{m_1}{\sqrt{g g_{\rho\sigma} \frac{v_1^\rho v_1^\sigma}{c^2}}}\ v_1^\mu(t) v_1^\nu(t)\ \delta^3(\mathbf{x} - \mathbf{y}_1(t)) + 1 \leftrightarrow 2$$

This implies a divergence of the metric at the particles positions which is solved through the Hadamard regularization. [L. Blanchet, G. Faye, J. Math. Phys. 41 (2000) 7675]

Matter source

Consider a binary system of two black holes of masses m_1 and m_2. It is usually approximated by two point-like particles:

$$T^{\mu\nu}(\mathbf{x},t) = \frac{m_1}{\sqrt{g g_{\rho\sigma}\frac{v_1^\rho v_1^\sigma}{c^2}}}\; v_1^\mu(t) v_1^\nu(t)\; \delta^3(\mathbf{x}-\mathbf{y}_1(t)) + 1 \leftrightarrow 2$$

This implies a divergence of the metric at the particles positions which is solved through the Hadamard regularization. [L. Blanchet, G. Faye, J. Math. Phys. 41 (2000) 7675]

Useful parametrization:

- total mass: $M = m_1 + m_2$
- reduced mass: $\mu = \frac{m_1 m_2}{M}$
- symmetric mass ratio: $\nu = \frac{\mu}{M} = \frac{m_1 m_2}{M^2}$

The balance equation

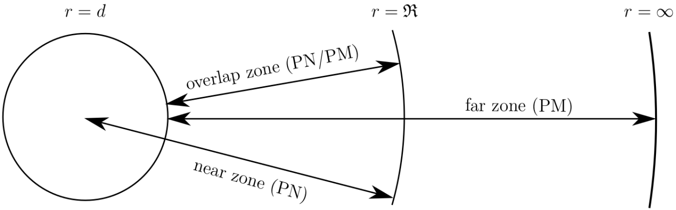

The balance equation

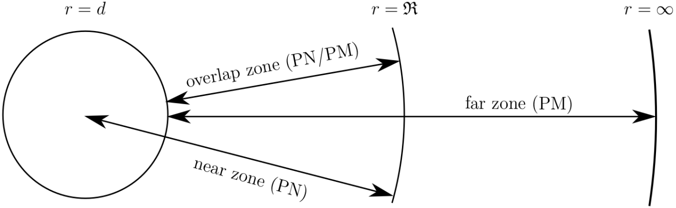

Equations of motion - energy E:

- $\nabla_\nu T^{\mu\nu} = 0$
- $\mathbf{a}_1 = -\frac{Gm_2}{r_{12}^2}\mathbf{n}_{12} + \mathcal{O}(2)$
- $E = \frac{m_1 v_1^2}{2} - \frac{Gm_1 m_2}{2r_{12}} + \mathcal{O}(2) + 1 \leftrightarrow 2$

The balance equation

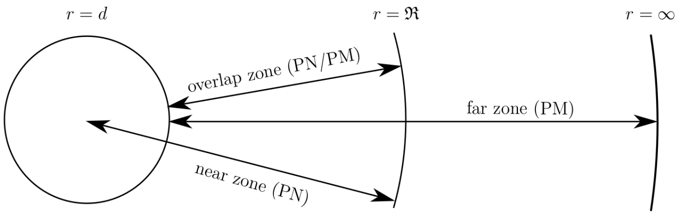

Equations of motion - energy E:

- $\nabla_\nu T^{\mu\nu} = 0$
- $\mathbf{a}_1 = -\frac{Gm_2}{r_{12}^2}\mathbf{n}_{12} + \mathcal{O}(2)$
- $E = \frac{m_1 v_1^2}{2} - \frac{Gm_1 m_2}{2r_{12}} + \mathcal{O}(2) + 1 \leftrightarrow 2$

Radiated flux $\mathcal{F}$:

- $\mathcal{F} = \frac{G}{c^5}\left(\frac{1}{5} I_{ij}^{(3)} I_{ij}^{(3)} + \mathcal{O}(2)\right)$
- $\mathcal{F} = \frac{G}{c^5}\left(\frac{32 G^3 M^5 \nu^2}{5 r^5} + \mathcal{O}(2)\right)$

The balance equation

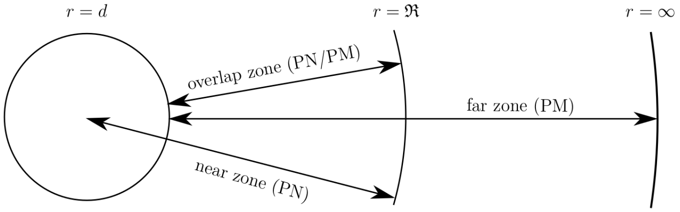

Equations of motion - energy E:

- $\nabla_\nu T^{\mu\nu} = 0$
- $\mathbf{a}_1 = -\frac{Gm_2}{r_{12}^2}\mathbf{n}_{12} + \mathcal{O}(2)$
- $E = \frac{m_1 v_1^2}{2} - \frac{Gm_1 m_2}{2r_{12}} + \mathcal{O}(2) + 1 \leftrightarrow 2$

Radiated flux $\mathcal{F}$:

- $\mathcal{F} = \frac{G}{c^5}\left(\frac{1}{5} I_{ij}^{(3)} I_{ij}^{(3)} + \mathcal{O}(2)\right)$
- $\mathcal{F} = \frac{G}{c^5}\left(\frac{32 G^3 M^5 \nu^2}{5 r^5} + \mathcal{O}(2)\right)$

Conservation of energy implies the balance equation and the orbital phase:

$$\frac{dE}{dt} = -\mathcal{F} \quad \Rightarrow \quad \phi = \int \Omega(t) dt$$

Quasi-circular orbit

The orbit of most binary systems has been circularized at the stage they enter the detectors bandwidth:

$$\dot{r} = \mathbf{n} \cdot \mathbf{v} = \mathcal{O}(5)$$

Quasi-circular orbit

The orbit of most binary systems has been circularized at the stage they enter the detectors bandwidth:

$$\dot{r} = \mathbf{n} \cdot \mathbf{v} = \mathcal{O}(5)$$

The equations of motion simplifies:

$$\mathbf{a} = -\Omega^2 \mathbf{x} + \mathcal{O}(5)$$

Quasi-circular orbit

The orbit of most binary systems has been circularized at the stage they enter the detectors bandwidth:

$$\dot{r} = \mathbf{n} \cdot \mathbf{v} = \mathcal{O}(5)$$

The equations of motion simplifies:

$$\mathbf{a} = -\Omega^2 \mathbf{x} + \mathcal{O}(5)$$

with the orbital frequency

$$\Omega^2 = \frac{GM}{r^3}\left[1 + (-3+\nu)\gamma + \left(6 + \frac{41}{4}\nu + \nu^2\right)\gamma^2\right] + \mathcal{O}(5)$$

where

$$\gamma = \frac{GM}{rc^2}.$$

State-of-the-art computations

For data analysis, consider the waveform in frequency space:

$$h(f) = A(f)\, e^{i\psi(f)}.$$

State-of-the-art computations

For data analysis, consider the waveform in frequency space:

$$h(f) = A(f)\, e^{i\psi(f)}.$$

The phase $\psi(f)$ (Fourier transform of $\phi(t)$) has been calculated to 3.5PN accuracy:

$$\psi(f) = 2\pi f t_c - \phi_c - \frac{\pi}{4} + \frac{3}{128} \sum_{j=0}^{7} \varphi_j \left(\frac{\pi M G f}{c^3} \right)^{(j-5)/3},$$

State-of-the-art computations

For data analysis, consider the waveform in frequency space:

$$h(f) = A(f)\, e^{i\psi(f)}.$$

The phase $\psi(f)$ (Fourier transform of $\phi(t)$) has been calculated to 3.5PN accuracy:

$$\psi(f) = 2\pi f t_c - \phi_c - \frac{\pi}{4} + \frac{3}{128}\sum_{j=0}^{7} \varphi_j \left(\frac{\pi M G f}{c^3}\right)^{(j-5)/3},$$

where the phase coefficients are

$$\begin{aligned}
\varphi_0 &= 1 \\
\varphi_1 &= 0 \\
\varphi_2 &= \tfrac{3715}{756} + \tfrac{55}{9}\nu \\
\varphi_3 &= -16\pi \\
\varphi_4 &= \tfrac{15293365}{508032} + \tfrac{27145}{504}\nu + \tfrac{3085}{72}\nu^2 \\
&\dots
\end{aligned}$$

[T. Damour, B. Iyer and B. Sathyaprakash, Phys. Rev. D 63 (2001) 044023]

[G. Faye, S. Marsat, L. Blanchet, B. Iyer, Class. Quantum Grav. 29 (2012) 175004]

GR vs. GW150914

Pictorial representation on simulated data

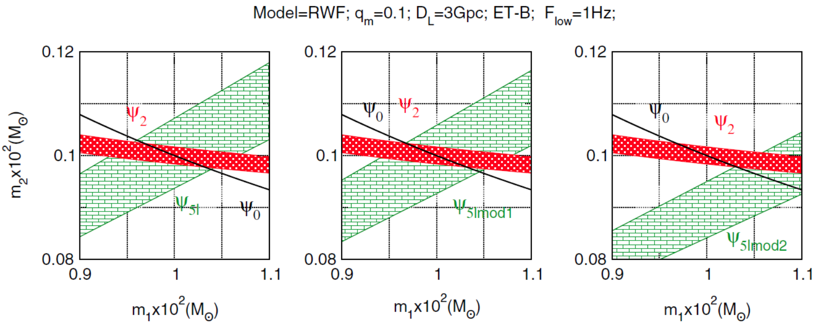

[C. Mishra, K. Arun, B. Iyer, B. Sathyaprakash, Phys. Rev. D 82 (2010) 064010]

Bayesian analysis from GW150914

waveform regime	parameter	f−dependence	median single	median multiple	GR quantile single	GR quantile multiple	$\log_{10} B^{GR}_{model}$ single	$\log_{10} B^{GR}_{model}$ multiple
early-inspiral regime	$\delta\hat{\varphi}_0$	$f^{-5/3}$	$-0.1^{+0.1}_{-0.1}$	$1.3^{+3.0}_{-3.2}$	0.94	0.30	1.9 ± 0.2	3.7 ± 0.6
	$\delta\hat{\varphi}_1$	$f^{-4/3}$	$0.3^{+0.4}_{-0.4}$	$-0.5^{+0.6}_{-0.6}$	0.16	0.93	1.6 ± 0.2	
	$\delta\hat{\varphi}_2$	f^{-1}	$-0.4^{+0.3}_{-0.4}$	$-1.6^{+18.8}_{-16.6}$	0.96	0.56	1.2 ± 0.2	
	$\delta\hat{\varphi}_3$	$f^{-2/3}$	$0.2^{+0.2}_{-0.2}$	$2.0^{+13.4}_{-13.9}$	0.02	0.42	1.2 ± 0.2	
	$\delta\hat{\varphi}_4$	$f^{-1/3}$	$-1.9^{+1.6}_{-1.7}$	$-1.9^{+19.3}_{-16.4}$	0.98	0.56	0.3 ± 0.2	
	$\delta\hat{\varphi}_{5l}$	$\log(f)$	$0.8^{+0.5}_{-0.6}$	$-1.4^{+18.6}_{-16.9}$	0.01	0.55	0.7 ± 0.4	
	$\delta\hat{\varphi}_6$	$f^{1/3}$	$-1.4^{+1.1}_{-1.1}$	$1.2^{+16.8}_{-18.9}$	0.99	0.47	0.4 ± 0.2	
	$\delta\hat{\varphi}_{6l}$	$f^{1/3}\log(f)$	$8.9^{+6.8}_{-6.8}$	$-1.9^{+19.1}_{-16.1}$	0.02	0.57	-0.3 ± 0.2	
	$\delta\hat{\varphi}_7$	$f^{2/3}$	$3.8^{+2.9}_{-2.9}$	$3.2^{+15.1}_{-19.2}$	0.02	0.41	-0.0 ± 0.2	
intermediate regime	$\delta\hat{\beta}_2$	$\log f$	$0.1^{+0.4}_{-0.3}$	$0.2^{+0.6}_{-0.5}$	0.24	0.28	1.4 ± 0.2	2.3 ± 0.2
	$\delta\hat{\beta}_3$	f^{-3}	$0.1^{+0.6}_{-0.3}$	$-0.0^{+0.8}_{-0.7}$	0.31	0.56	1.2 ± 0.4	
merger-ringdown regime	$\delta\hat{\alpha}_2$	f^{-1}	$-0.1^{+0.4}_{-0.4}$	$0.0^{+1.0}_{-1.2}$	0.68	0.50	1.2 ± 0.2	2.1 ± 0.4
	$\delta\hat{\alpha}_3$	$f^{3/4}$	$-0.3^{+1.9}_{-1.5}$	$0.0^{+4.4}_{-4.4}$	0.60	0.51	0.7 ± 0.2	
	$\delta\hat{\alpha}_4$	$\tan^{-1}(af+b)$	$-0.1^{+0.5}_{-0.5}$	$-0.1^{+1.1}_{-1.0}$	0.68	0.62	1.1 ± 0.2	

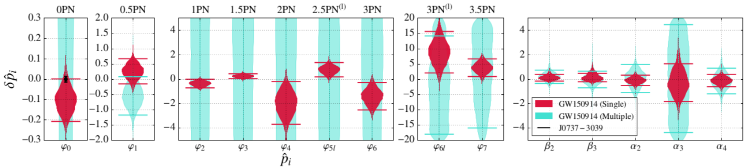

[LIGO/Virgo Coll., Phys. Rev. Lett. 116 (2016) 221101]

Noncommutative corrections to the waveform

A. Kobakhidze, CL, A. Manning, PRD 94 (2016) 064033

Noncommutative space-time

NC space-time arises in a number of contexts:

- Originally proposed by Heisenberg as an effective UV cutoff.
- Formalization by Snyder [Phys. Rev. 71 (1947) 38].
- Noncommutative geometry [A. Connes, Inst. Hautes Etudes Sci. Publ. Math. 62 (1985) 257].
- Low-energy limit of string theory [N. Seiberg and E.Witten, JHEP 9909 (1999) 032].

Noncommutative space-time

NC space-time arises in a number of contexts:

- Originally proposed by Heisenberg as an effective UV cutoff.
- Formalization by Snyder [Phys. Rev. 71 (1947) 38].
- Noncommutative geometry [A. Connes, Inst. Hautes Etudes Sci. Publ. Math. 62 (1985) 257].
- Low-energy limit of string theory [N. Seiberg and E.Witten, JHEP 9909 (1999) 032].

We focus on the canonical algebra of coordinates:

$$[\hat{x}^\mu, \hat{x}^\nu] = i\theta^{\mu\nu} \qquad \Delta x^\mu \Delta x^\nu \geq \frac{1}{2}|\theta^{\mu\nu}|$$

Noncommutative space-time

NC space-time arises in a number of contexts:

- Originally proposed by Heisenberg as an effective UV cutoff.
- Formalization by Snyder [Phys. Rev. 71 (1947) 38].
- Noncommutative geometry [A. Connes, Inst. Hautes Etudes Sci. Publ. Math. 62 (1985) 257].
- Low-energy limit of string theory [N. Seiberg and E.Witten, JHEP 9909 (1999) 032].

We focus on the canonical algebra of coordinates:

$$[\hat{x}^\mu, \hat{x}^\nu] = i\theta^{\mu\nu} \qquad \Delta x^\mu \Delta x^\nu \geq \frac{1}{2}|\theta^{\mu\nu}|$$

Previous constraints on noncommutative scale at inverse $\sim$ TeV.

[S. Carroll et al., Phys. Rev. Lett.87 (2001) 141601] [X. Calmet, Eur. Phys. J. C41 (2005) 269]

Noncommutative space-time

NC space-time arises in a number of contexts:

- Originally proposed by Heisenberg as an effective UV cutoff.
- Formalization by Snyder [Phys. Rev. 71 (1947) 38].
- Noncommutative geometry [A. Connes, Inst. Hautes Etudes Sci. Publ. Math. 62 (1985) 257].
- Low-energy limit of string theory [N. Seiberg and E.Witten, JHEP 9909 (1999) 032].

We focus on the canonical algebra of coordinates:

$$[\hat{x}^\mu, \hat{x}^\nu] = i\theta^{\mu\nu} \qquad \Delta x^\mu \Delta x^\nu \geq \frac{1}{2}|\theta^{\mu\nu}|$$

Previous constraints on noncommutative scale at inverse $\sim$ TeV.

[S. Carroll et al., Phys. Rev. Lett.87 (2001) 141601] [X. Calmet, Eur. Phys. J. C41 (2005) 269]

Noncommutative QFT - fields product replaced by Moyal product:

$$f(x) \star g(x) = f(x)g(x) + \sum_{n=1}^{+\infty} \left(\frac{i}{2}\right)^n \frac{1}{n!} \theta^{\alpha_1 \beta 1} \cdots \theta^{\alpha_n \beta_n} \, \partial_{\alpha_1} \cdots \partial_{\alpha_n} f(x) \, \partial_{\beta_1} \cdots \partial_{\beta_n} g(x)$$

Noncommutative effects on GWs

Expect both modifications on the matter source and on the EFE.

Expect both modifications on the matter source and on the EFE.

- Consider a Schwarzschild black hole described by a massive scalar field in noncommutative QFT[A. Kobakhidze, Phys. Rev. D79 (2009) 047701]:

$$T^{\mu\nu}_{NC}(x) = \frac{1}{2}\left(\partial^\mu\phi\star\partial^\nu\phi + \partial^\nu\phi\star\partial^\mu\phi\right) - \frac{1}{2}\eta^{\mu\nu}\left(\partial_\rho\phi\star\partial^\rho\phi - m^2\phi\star\phi\right)$$

Similar approach as for the quantum corrections of a Schwarzschild BH.

[N. E. J. Bjerrum-Bohr, J. F. Donoghue, B. R. Holstein, Phys. Rev. D68 (2003) 084005]

Expect both modifications on the matter source and on the EFE.

- Consider a Schwarzschild black hole described by a massive scalar field in noncommutative QFT[A. Kobakhidze, Phys. Rev. D79 (2009) 047701]:

$$T^{\mu\nu}_{NC}(x) = \frac{1}{2}\left(\partial^\mu\phi \star \partial^\nu\phi + \partial^\nu\phi \star \partial^\mu\phi\right) - \frac{1}{2}\eta^{\mu\nu}\left(\partial_\rho\phi \star \partial^\rho\phi - m^2\phi \star \phi\right)$$

  Similar approach as for the quantum corrections of a Schwarzschild BH.

  [N. E. J. Bjerrum-Bohr, J. F. Donoghue, B. R. Holstein, Phys. Rev. D68 (2003) 084005]

- Neglect corrections to the laws of GR, since noncommutative gravity appears at $\mathcal{O}(|\theta|^2)$ and is model-dependent.

  [X. Calmet, A. Kobakhidze, Phys. Rev. D74 (2006) 047702] [P. Mukherjee, A. Saha, Phys. Rev. D74 (2006) 027702]

Energy-momentum tensor in noncommutative space-time

After quantising and keeping leading-order corrections of the Moyal product:

$$T^{\mu\nu}_{NC}(\mathbf{x},t) \approx T^{\mu\nu}_{GR}(\mathbf{x},t) + \frac{m^3 G^2}{8c^4} v^\mu v^\nu \Theta^{kl} \partial_k \partial_l \, \delta^3(\mathbf{x} - \mathbf{y}(t))$$

with

$$\Theta^{kl} = \frac{\theta^{0k}\theta^{0l}}{l_P^2 t_P^2} + 2\frac{v_p}{c}\frac{\theta^{0k}\theta^{pl}}{l_P^3 t_P} + \frac{v_p v_q}{c^2}\frac{\theta^{kp}\theta^{lq}}{l_P^4} = \frac{\theta^{0k}\theta^{0l}}{l_P^2 t_P^2} + \mathcal{O}(1)$$

Energy-momentum tensor in noncommutative space-time

After quantising and keeping leading-order corrections of the Moyal product:

$$T^{\mu\nu}_{NC}(\mathbf{x},t) \approx T^{\mu\nu}_{GR}(\mathbf{x},t) + \frac{m^3G^2}{8c^4} v^\mu v^\nu \Theta^{kl} \partial_k \partial_l \, \delta^3(\mathbf{x} - \mathbf{y}(t))$$

with

$$\Theta^{kl} = \frac{\theta^{0k}\theta^{0l}}{l_P^2 t_P^2} + 2\frac{v_p}{c}\frac{\theta^{0k}\theta^{pl}}{l_P^3 t_P} + \frac{v_p v_q}{c^2}\frac{\theta^{kp}\theta^{lq}}{l_P^4} = \frac{\theta^{0k}\theta^{0l}}{l_P^2 t_P^2} + \mathcal{O}(1)$$

Binary black hole EMT with 2PN noncommutative corrections:

$$T^{\mu\nu}(\mathbf{x},t) = m_1\gamma_1 v_1^\mu v_1^\nu \delta^3(\mathbf{x} - \mathbf{y}_1(t)) + \frac{m_1^3 G^2 \kappa^2}{8c^4} v_1^\mu v_1^\nu \theta^k \theta^l \partial_k \partial_l \, \delta^3(\mathbf{x} - \mathbf{y}_1(t)) + 1 \leftrightarrow 2$$

where

$$\kappa\theta^i = \frac{\theta^{0i}}{l_P t_P}.$$

The modified balance equation

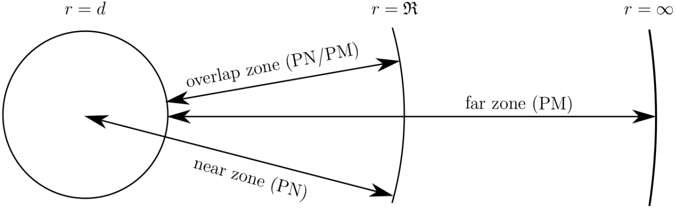

$$\frac{d(E + E_{NC})}{dt} = -\mathcal{F} - \mathcal{F}_{NC}$$

2PN noncommutative correction to the energy

Conservation of the energy-momentum tensor, $\nabla_\nu T^{\mu\nu} = 0$:

$$a_i = (a_i)^{2PN}_{GR} - \frac{15M^3(1-2\nu)G^3\kappa^2}{8c^4r^4}\theta^k\theta^l\hat{n}_{ikl} + \mathcal{O}(5),$$

$$E = E^{2PN}_{GR} - \frac{3M^3\mu(1-2\nu)G^3\kappa^2}{8c^4r^3}\theta^k\theta^l\hat{n}_{kl} + \mathcal{O}(5).$$

2PN noncommutative correction to the energy

Conservation of the energy-momentum tensor, $\nabla_\nu T^{\mu\nu} = 0$:

$$a_i = (a_i)^{2PN}_{GR} - \frac{15M^3(1-2\nu)G^3\kappa^2}{8c^4r^4}\theta^k\theta^l\hat{n}_{ikl} + \mathcal{O}(5),$$

$$E = E^{2PN}_{GR} - \frac{3M^3\mu(1-2\nu)G^3\kappa^2}{8c^4r^3}\theta^k\theta^l\hat{n}_{kl} + \mathcal{O}(5).$$

Effect of a preferred direction $\boldsymbol{\theta}$:

$$\theta^k\theta^l\hat{n}_{ikl} = n_i\left(\mathbf{n}\cdot\boldsymbol{\theta}\right)^2 - \frac{1}{5}n_i - \frac{2}{5}\theta_i\left(\mathbf{n}\cdot\boldsymbol{\theta}\right),$$

$$\theta^k\theta^l\hat{n}_{kl} = \left(\mathbf{n}\cdot\boldsymbol{\theta}\right)^2 - \frac{1}{3}.$$

2PN noncommutative correction to the energy

Conservation of the energy-momentum tensor, $\nabla_\nu T^{\mu\nu} = 0$:

$$a_i = (a_i)_{GR}^{2PN} - \frac{15M^3(1-2\nu)G^3\kappa^2}{8c^4r^4}\theta^k\theta^l\hat{n}_{ikl} + \mathcal{O}(5),$$

$$E = E_{GR}^{2PN} - \frac{3M^3\mu(1-2\nu)G^3\kappa^2}{8c^4r^3}\theta^k\theta^l\hat{n}_{kl} + \mathcal{O}(5).$$

Effect of a preferred direction $\boldsymbol{\theta}$:

$$\theta^k\theta^l\hat{n}_{ikl} = n_i\,(\mathbf{n}\cdot\boldsymbol{\theta})^2 - \frac{1}{5}n_i - \frac{2}{5}\theta_i\,(\mathbf{n}\cdot\boldsymbol{\theta})\,,$$

$$\theta^k\theta^l\hat{n}_{kl} = (\mathbf{n}\cdot\boldsymbol{\theta})^2 - \frac{1}{3}.$$

For simplicity (we only look for a bound on κ), we neglect the "modulation terms" in $\mathbf{n}\cdot\boldsymbol{\theta}$.

2PN noncommutative correction to the flux and the phase

Correction to the multipole formula:

$$\mathcal{F} = \frac{G}{c^5}\left(\frac{1}{5} I_{ij}^{(3)} I_{ij}^{(3)} + \mathcal{O}(2)\right)$$

$$\mathcal{F}_{NC} = \frac{G}{c^5}\left(-\frac{36}{5}\frac{G^5 M^7}{c^4 r^7}\nu^2(1-2\nu)\kappa^2 + \mathcal{O}(5)\right)$$

2PN noncommutative correction to the flux and the phase

Correction to the multipole formula:

$$\mathcal{F} = \frac{G}{c^5}\left(\frac{1}{5} I_{ij}^{(3)} I_{ij}^{(3)} + \mathcal{O}(2)\right)$$

$$\mathcal{F}_{NC} = \frac{G}{c^5}\left(-\frac{36}{5}\frac{G^5 M^7}{c^4 r^7}\nu^2(1-2\nu)\kappa^2 + \mathcal{O}(5)\right)$$

From E, $\mathcal{F}$ and the balance equation:

$$\varphi_4 = \frac{15293365}{508032} + \frac{27145}{504}\nu + \frac{3085}{72}\nu^2 + \frac{5}{4}(1-2\nu)\kappa^2$$

Constraint on the scale of noncommutativity

Noncommutativity vs. GW150914

waveform regime	parameter	$f-$dependence	median single	median multiple	GR quantile single	GR quantile multiple	$\log_{10} B^{\mathrm{GR}}_{\mathrm{model}}$ single	$\log_{10} B^{\mathrm{GR}}_{\mathrm{model}}$ multiple
early-inspiral regime	$\delta\hat{\varphi}_0$	$f^{-5/3}$	$-0.1^{+0.1}_{-0.1}$	$1.3^{+3.0}_{-3.2}$	0.94	0.30	1.9 ± 0.2	3.7 ± 0.6
	$\delta\hat{\varphi}_1$	$f^{-4/3}$	$0.3^{+0.4}_{-0.4}$	$-0.5^{+0.6}_{-0.6}$	0.16	0.93	1.6 ± 0.2	
	$\delta\hat{\varphi}_2$	f^{-1}	$-0.4^{+0.3}_{-0.4}$	$-1.6^{+18.8}_{-16.6}$	0.96	0.56	1.2 ± 0.2	
	$\delta\hat{\varphi}_3$	$f^{-2/3}$	$0.2^{+0.2}_{-0.2}$	$2.0^{+13.4}_{-13.9}$	0.02	0.42	1.2 ± 0.2	
	$\delta\hat{\varphi}_4$	$f^{-1/3}$	$-1.9^{+1.6}_{-1.7}$	$-1.9^{+19.3}_{-16.4}$	0.98	0.56	0.3 ± 0.2	
	$\delta\hat{\varphi}_{5l}$	$\log(f)$	$0.8^{+0.5}_{-0.6}$	$-1.4^{+18.6}_{-16.9}$	0.01	0.55	0.7 ± 0.4	
	$\delta\hat{\varphi}_6$	$f^{1/3}$	$-1.4^{+1.1}_{-1.1}$	$1.2^{+16.8}_{-18.9}$	0.99	0.47	0.4 ± 0.2	
	$\delta\hat{\varphi}_{6l}$	$f^{1/3}\log(f)$	$8.9^{+6.8}_{-6.8}$	$-1.9^{+19.1}_{-16.1}$	0.02	0.57	-0.3 ± 0.2	
	$\delta\hat{\varphi}_7$	$f^{2/3}$	$3.8^{+2.9}_{-2.9}$	$3.2^{+15.1}_{-19.2}$	0.02	0.41	-0.0 ± 0.2	
intermediate regime	$\delta\hat{\beta}_2$	$\log f$	$0.1^{+0.4}_{-0.3}$	$0.2^{+0.6}_{-0.5}$	0.24	0.28	1.4 ± 0.2	2.3 ± 0.2
	$\delta\hat{\beta}_3$	f^{-3}	$0.1^{+0.6}_{-0.3}$	$-0.0^{+0.8}_{-0.7}$	0.31	0.56	1.2 ± 0.4	
merger-ringdown regime	$\delta\hat{\alpha}_2$	f^{-1}	$-0.1^{+0.4}_{-0.4}$	$0.0^{+1.0}_{-1.2}$	0.68	0.50	1.2 ± 0.2	2.1 ± 0.4
	$\delta\hat{\alpha}_3$	$f^{3/4}$	$-0.3^{+1.9}_{-1.5}$	$0.0^{+4.4}_{-4.4}$	0.60	0.51	0.7 ± 0.2	
	$\delta\hat{\alpha}_4$	$\tan^{-1}(af+b)$	$-0.1^{+0.5}_{-0.5}$	$-0.1^{+1.1}_{-1.0}$	0.68	0.62	1.1 ± 0.2	

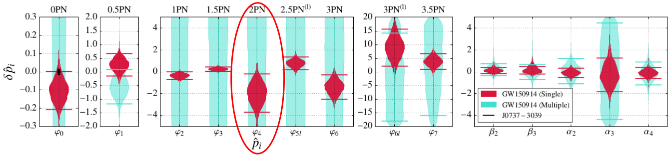

$$\delta\varphi_4^{NC} = \frac{\varphi_4^{NC}}{\varphi_4^{GR}} = \frac{1270080\,(1-2\nu)}{4353552\,\nu^2 + 5472432\,\nu + 3058673}\kappa^2$$

$$|\delta\varphi_4^{NC}| \lesssim 20 \Rightarrow \sqrt{\kappa} \lesssim 3.5$$

Summary of Part I

- Several observations of binary system merger by LIGO/Virgo

Summary of Part I

- Several observations of binary system merger by LIGO/Virgo
- GW waveform consistent with GR

Summary of Part I

- Several observations of binary system merger by LIGO/Virgo
- GW waveform consistent with GR
- Derivation of the lowest-order (2PN) noncommutative correction to the GW waveform.

Summary of Part I

- Several observations of binary system merger by LIGO/Virgo
- GW waveform consistent with GR
- Derivation of the lowest-order (2PN) noncommutative correction to the GW waveform.
- Constraint on the scale of noncommutativity to around the Planck scale:

$$|\theta^{0i}| \lesssim 12 \cdot l_P t_P$$

Part II: Phase transitions and Gravitational Waves

First-order phase transition and GWs

Hot Big Bang scenario:

- early Universe $\sim$ hot plasma (high T)
- scalar field(s) behaviour dictated by their free energy density $\mathcal{F}(\rho, T)$
- depends on the underlying particle physics model

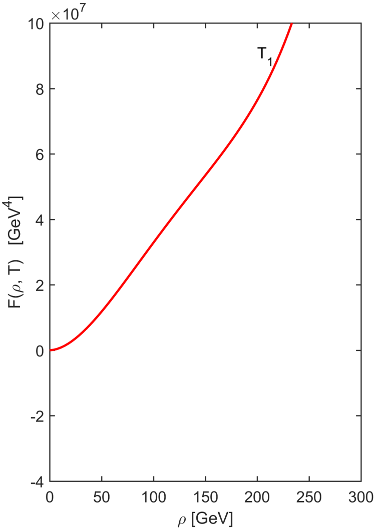

First-order phase transition and GWs

Hot Big Bang scenario:

- early Universe $\sim$ hot plasma (high T)
- scalar field(s) behaviour dictated by their free energy density $\mathcal{F}(\rho, T)$
- depends on the underlying particle physics model

1st-order phase transition:

- bubble nucleation
- bubble collision
- stochastic GW background

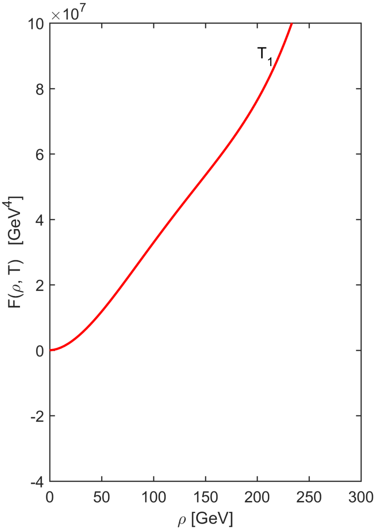

First-order phase transition and GWs

Hot Big Bang scenario:

- early Universe $\sim$ hot plasma (high T)
- scalar field(s) behaviour dictated by their free energy density $\mathcal{F}(\rho, T)$
- depends on the underlying particle physics model

1st-order phase transition:

- bubble nucleation
- bubble collision
- stochastic GW background

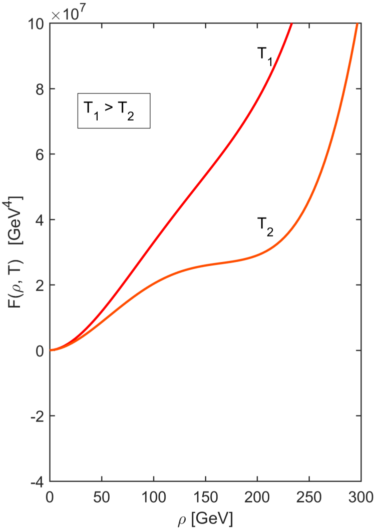

First-order phase transition and GWs

Hot Big Bang scenario:

- early Universe $\sim$ hot plasma (high T)
- scalar field(s) behaviour dictated by their free energy density $\mathcal{F}(\rho, T)$
- depends on the underlying particle physics model

1st-order phase transition:

- bubble nucleation
- bubble collision
- stochastic GW background

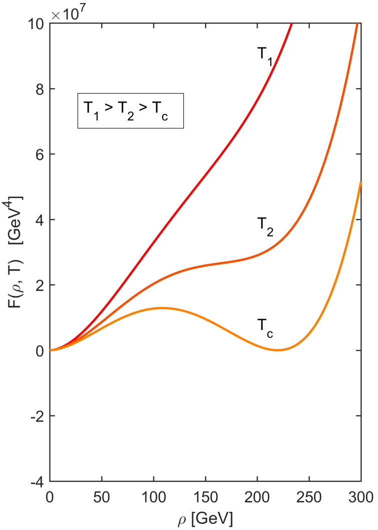

First-order phase transition and GWs

Hot Big Bang scenario:

- early Universe $\sim$ hot plasma (high T)
- scalar field(s) behaviour dictated by their free energy density $\mathcal{F}(\rho, T)$
- depends on the underlying particle physics model

1st-order phase transition:

- bubble nucleation
- bubble collision
- stochastic GW background

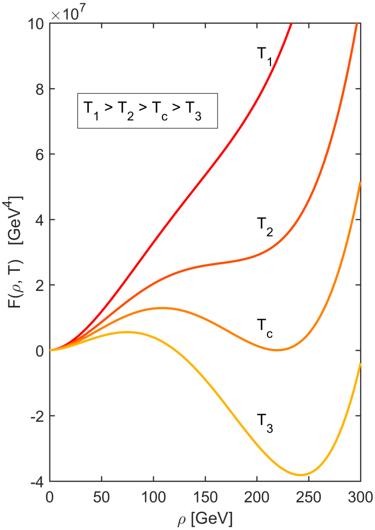

Example: one of the latest simulation

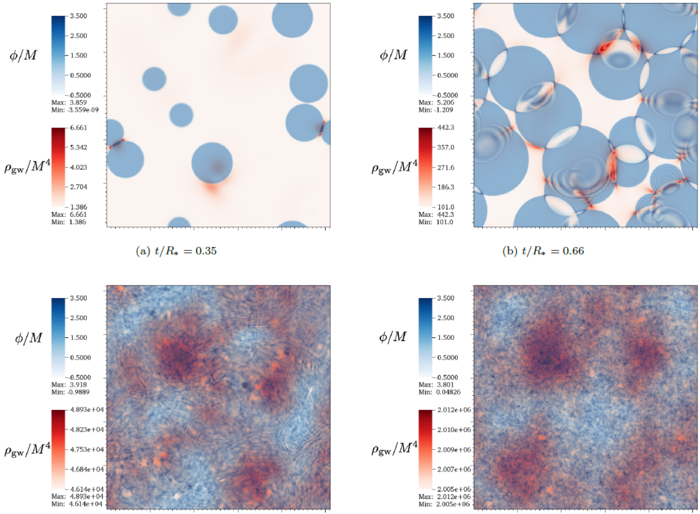

(a) $t/R_* = 0.35$ (b) $t/R_* = 0.66$

(c) $t/R_* = 2.50$ (d) $t/R_* = 7.8$

[D. Cutting, M. Hindmarsh, D. Weir, arXiv:1802.05712]

(B)SM and GW detection

A possible probe of new physics:

- no 1st-order PT in the Standard Model [K. Kajantie et al., Phys. Rev. Lett. 77 (1996) 2887]

  $\Rightarrow$ no stochastic GW background predicted in the SM

- various BSM models account for a 1st-order EWPT (e.g. motivated by electroweak baryogenesis)

(B)SM and GW detection

A possible probe of new physics:

- no 1st-order PT in the Standard Model [K. Kajantie et al., Phys. Rev. Lett. 77 (1996) 2887]

  $\Rightarrow$ no stochastic GW background predicted in the SM

- various BSM models account for a 1st-order EWPT (e.g. motivated by electroweak baryogenesis)

GW detection:

- background peak frequency vs. detectors sensitivity band

- common scenario: EWPT around $T_{EW} \sim 100$ GeV

  $\Rightarrow f_{\text{peak}} \sim$ milliHertz $\Rightarrow$ range of eLISA [C. Caprini et al., JCAP 1604 (2016) no.04 001]

- we discuss here a prolonged EWPT $\Rightarrow f_{\text{peak}} \sim 10^{-8}$ Hz

  $\Rightarrow$ range of pulsar timing arrays (EPTA, SKA,...)

(B)SM and GW detection

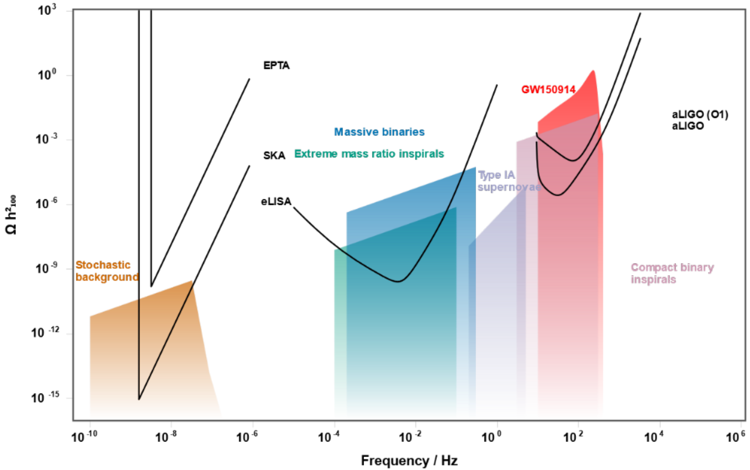

[From rhcole.com/apps/GWplotter/]

A model: non-linearly realised electroweak gauge group

Realisation of $SU(2)_L \times U(1)_Y$

Main idea:

- $\mathcal{G}_{\text{coset}} = SU(2)_L \times U(1)_Y / U(1)_Q$ is gauged
- with broken generators $T^i = \sigma^i - \delta^{i3}\mathbb{I}$ and Goldstone bosons $\pi^i(x)$
- physical Higgs as a singlet $\rho(x) \sim (\mathbf{1},\mathbf{1})_0$

Realisation of $SU(2)_L \times U(1)_Y$

Main idea:

- $\mathcal{G}_{\text{coset}} = SU(2)_L \times U(1)_Y / U(1)_Q$ is gauged
- with broken generators $T^i = \sigma^i - \delta^{i3}\mathbb{I}$ and Goldstone bosons $\pi^i(x)$
- physical Higgs as a singlet $\rho(x) \sim (\mathbf{1}, \mathbf{1})_0$

SM Higgs doublet identified as $H(x) = \frac{\rho(x)}{\sqrt{2}} e^{\frac{i}{2}\pi^i(x) T^i} \begin{pmatrix} 0 \\ 1 \end{pmatrix}, \qquad i \in \{1, 2, 3\}$

Realisation of $SU(2)_L \times U(1)_Y$

Main idea:

- $\mathcal{G}_{\text{coset}} = SU(2)_L \times U(1)_Y / U(1)_Q$ is gauged
- with broken generators $T^i = \sigma^i - \delta^{i3}\mathbb{I}$ and Goldstone bosons $\pi^i(x)$
- physical Higgs as a singlet $\rho(x) \sim (\mathbf{1}, \mathbf{1})_0$

SM Higgs doublet identified as $H(x) = \frac{\rho(x)}{\sqrt{2}} e^{\frac{i}{2}\pi^i(x) T^i} \begin{pmatrix} 0 \\ 1 \end{pmatrix}, \qquad i \in \{1, 2, 3\}$

SM particle content but BSM interactions

Realisation of $SU(2)_L \times U(1)_Y$

Main idea:

- $\mathcal{G}_{\text{coset}} = SU(2)_L \times U(1)_Y / U(1)_Q$ is gauged
- with broken generators $T^i = \sigma^i - \delta^{i3}\mathbb{I}$ and Goldstone bosons $\pi^i(x)$
- physical Higgs as a singlet $\rho(x) \sim (\mathbf{1}, \mathbf{1})_0$

SM Higgs doublet identified as $H(x) = \frac{\rho(x)}{\sqrt{2}} e^{\frac{i}{2}\pi^i(x)T^i} \begin{pmatrix} 0 \\ 1 \end{pmatrix}, \qquad i \in \{1,2,3\}$

SM particle content but BSM interactions

Minimal setup (usual SM configurations except Higgs potential):

$$V^{(0)}(\rho) = -\frac{\mu^2}{2}\rho^2 + \frac{\kappa}{3}\rho^3 + \frac{\lambda}{4}\rho^4.$$

Realisation of $SU(2)_L \times U(1)_Y$

Main idea:

- $\mathcal{G}_{\text{coset}} = SU(2)_L \times U(1)_Y / U(1)_Q$ is gauged
- with broken generators $T^i = \sigma^i - \delta^{i3}\mathbb{I}$ and Goldstone bosons $\pi^i(x)$
- physical Higgs as a singlet $\rho(x) \sim (\mathbf{1},\mathbf{1})_0$

SM Higgs doublet identified as $H(x) = \frac{\rho(x)}{\sqrt{2}} e^{\frac{i}{2}\pi^i(x)T^i} \begin{pmatrix} 0 \\ 1 \end{pmatrix}, \qquad i \in \{1,2,3\}$

SM particle content but BSM interactions

Minimal setup (usual SM configurations except Higgs potential):

$$V^{(0)}(\rho) = -\frac{\mu^2}{2}\rho^2 + \frac{\kappa}{3}\rho^3 + \frac{\lambda}{4}\rho^4.$$

For additional details, see e.g.: [M. Gonzalez-Alonso et al., Eur. Phys. J. C 75 (2015) 3, 128] [D. Binosi and A. Quadri, JHEP 1302 (2013) 020] [A. Kobakhidze, arXiv:1208.5180] [R. Contino et al., JHEP 1005 (2010) 089]

Early considerations

Model specified by one parameter: $\kappa = \bar{\kappa} \cdot \frac{m_h^2}{v} \sim 63.5 \cdot \bar{\kappa}$ GeV.

Barrier in the Higgs potential at tree level $\Rightarrow$ likely to allow a strong 1st-order EWPT.

Early considerations

Model specified by one parameter: $\kappa = \bar{\kappa} \cdot \frac{m_h^2}{v} \sim 63.5 \cdot \bar{\kappa}$ GeV.

Barrier in the Higgs potential at tree level $\Rightarrow$ likely to allow a strong 1st-order EWPT.

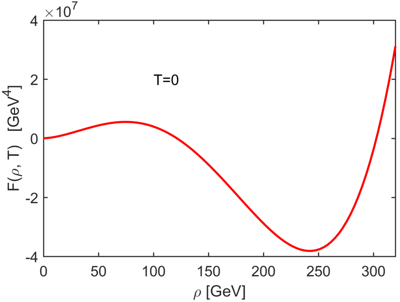

Early considerations

Model specified by one parameter: $\kappa = \bar{\kappa} \cdot \frac{m_h^2}{v} \sim 63.5 \cdot \bar{\kappa}$ GeV.

Barrier in the Higgs potential at tree level $\Rightarrow$ likely to allow a strong 1st-order EWPT.

Indeed confirmed by a previous study [A. Kobakhidze, A. Manning, J. Yue, arXiv:1607.00883]:

$$|\bar{\kappa}| \in [1.75, 1.85] \Rightarrow \text{GW signal detectable by eLISA}$$

General observation: higher $|\bar{\kappa}| \Rightarrow$ lower bubble nucleation probability

However, unclear process at $|\bar{\kappa}| \sim 1.9$

Prolonged electroweak phase transition

A. Kobakhidze, CL, A. Manning, J. Yue [arXiv:1703.06552]

Qualitative description

Standard scenario (quick PT):

- $\mathcal{O}(1)$ bubbles produced per Hubble volume at $T_n \lesssim T_{EW}$
- they rapidly collide $\Rightarrow$ percolation temperature $T_p \sim T_n$
- time scale of the process much shorter than Hubble time

Qualitative description

Standard scenario (quick PT):

- $\mathcal{O}(1)$ bubbles produced per Hubble volume at $T_n \lesssim T_{EW}$
- they rapidly collide $\Rightarrow$ percolation temperature $T_p \sim T_n$
- time scale of the process much shorter than Hubble time

Long-lasting and supercooled scenario:

- weaker nucleation probability
- less bubbles produced $\Rightarrow$ more time needed for them to collide
- $\Rightarrow T_p \ll T_n \lesssim T_{EW}$
- requires to take into account expansion of the Universe and to check low-temperature nucleation probability

Bubble nucleation probability

Decay probability per unit volume per unit time: $\Gamma(T) \approx A(T)e^{-S(T)}$ [A. Linde, Nucl. Phys. B216 (1983) 421]

Bubble nucleation probability

Decay probability per unit volume per unit time: $\Gamma(T) \approx A(T)e^{-S(T)}$ [A. Linde, Nucl. Phys. B216 (1983) 421]

Computation of the Euclidean action:

$$S[\rho, T] = 4\pi \int_0^\beta d\tau \int_0^\infty dr\; r^2 \left[\frac{1}{2}\left(\frac{d\rho}{d\tau}\right)^2 + \frac{1}{2}\left(\frac{d\rho}{dr}\right)^2 + \mathcal{F}(\rho, T) \right]$$

$$\frac{\partial^2 \rho}{\partial \tau^2} + \frac{\partial^2 \rho}{\partial r^2} + \frac{2}{r}\frac{\partial \rho}{\partial r} - \frac{\partial \mathcal{F}}{\partial \rho}(\rho, T) = 0 \quad + \quad \text{boundary conditions}$$

$$S[\rho, T] \approx \begin{cases} S_4[\rho, T] = 2\pi^2 \int_0^\infty d\tilde{r}\; \tilde{r}^3 \left[\frac{1}{2}\left(\frac{d\rho}{d\tilde{r}}\right)^2 + \mathcal{F}(\rho, T) \right], T \ll R_0^{-1} \\ \frac{1}{T} S_3[\rho, T] = \frac{4\pi}{T} \int_0^\infty dr\; r^2 \left[\frac{1}{2}\left(\frac{d\rho}{dr}\right)^2 + \mathcal{F}(\rho, T) \right], T \gg R_0^{-1} \end{cases}$$

Bubble nucleation probability

Decay probability per unit volume per unit time: $\Gamma(T) \approx A(T)e^{-S(T)}$ [A. Linde, Nucl. Phys. B216 (1983) 421]

Some numerical results:

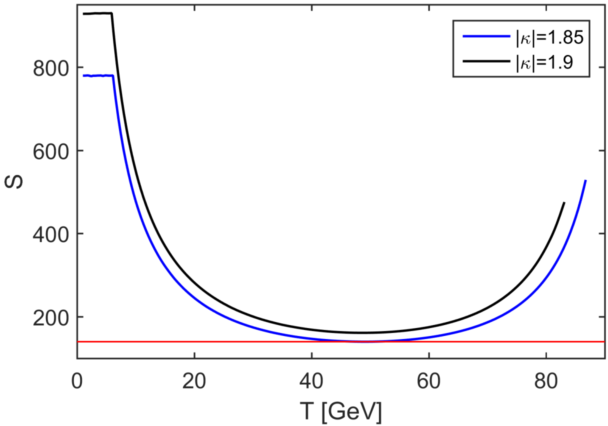

Standard scenario: number of bubbles $\sim \mathcal{O}(1)$ requires $\min S \lesssim 140$

Phase transition dynamics

General formalism in expanding universe: [M. Turner et al., Phys. Rev. D46 (1992) 2384].

Phase transition dynamics

General formalism in expanding universe: [M. Turner et al., Phys. Rev. D46 (1992) 2384].

Probability for a point of space-time to remain in the false-vacuum:

$$p(t) = \exp\left[-\frac{4\pi}{3}\int_{t_\star}^{t} dt'\Gamma(t')a^3(t')r^3(t,t')\right] \qquad r(t,t') = \int_{t'}^{t} dt'' \frac{v(t'')}{a(t'')}$$

Completion of the PT requires $p(t) \to 0$

Percolation temperature ($\sim$ collision) [L. Leitao et al., JCAP 1210 (2012) 024]: $p(t_p) \approx 0.7$

General formalism in expanding universe: [M. Turner et al., Phys. Rev. D46 (1992) 2384].

Probability for a point of space-time to remain in the false-vacuum:

$$p(t) = \exp\left[-\frac{4\pi}{3}\int_{t_\star}^{t} dt'\Gamma(t')a^3(t')r^3(t,t')\right] \qquad r(t,t') = \int_{t'}^{t} dt''\frac{v(t'')}{a(t'')}$$

Completion of the PT requires $p(t) \to 0$

Percolation temperature ($\sim$ collision) [L. Leitao et al., JCAP 1210 (2012) 024]: $p(t_p) \approx 0.7$

Number density of produced bubbles:

$$\frac{dN}{dR}(t,t_R) = \Gamma(t_R)\left(\frac{a(t_R)}{a(t)}\right)^4 \frac{p(t_R)}{v(t_R)}$$

Phase transition dynamics

General formalism in expanding universe: [M. Turner et al., Phys. Rev. D46 (1992) 2384].

Probability for a point of space-time to remain in the false-vacuum:

$$p(t) = \exp\left[-\frac{4\pi}{3}\int_{t_\star}^{t} dt'\Gamma(t')a^3(t')r^3(t,t')\right] \qquad r(t,t') = \int_{t'}^{t} dt'' \frac{v(t'')}{a(t'')}$$

Completion of the PT requires $p(t) \to 0$

Percolation temperature ($\sim$ collision) [L. Leitao et al., JCAP 1210 (2012) 024]: $p(t_p) \approx 0.7$

Number density of produced bubbles:

$$\frac{dN}{dR}(t,t_R) = \Gamma(t_R)\left(\frac{a(t_R)}{a(t)}\right)^4 \frac{p(t_R)}{v(t_R)}$$

Nucleation temperature T_n: maximum of $\frac{dN}{dR}(t_p, t_R)$

Bubbles properties at collision

By definition:

- most bubbles collide at t_p
- majority of them produced at t_n

$\Rightarrow$ bubble physical radius: $\bar{R} = a(t_p)r(t_p, t_n)$

Bubbles properties at collision

By definition:

- most bubbles collide at t_p
- majority of them produced at t_n

$\Rightarrow$ bubble physical radius: $\bar{R} = a(t_p) r(t_p, t_n)$

Kinetic energy stored in bubble-walls:

$$E_{\mathrm{kin}} = \kappa_\nu \cdot 4\pi \int_{t_n}^{t_p} dt \frac{dR}{dt}(t, t_n) R^2(t, t_n) \epsilon(t)$$

- $\epsilon(t)$: latent heat ($\sim$ vacuum energy)
- κ_ν: fraction of energy going into the wall motion (vs. heating the plasma)

Bubbles properties at collision

By definition:

- most bubbles collide at t_p
- majority of them produced at t_n

$\Rightarrow$ bubble physical radius: $\bar{R} = a(t_p)r(t_p, t_n)$

Kinetic energy stored in bubble-walls:

$$E_{\text{kin}} = \kappa_\nu \cdot 4\pi \int_{t_n}^{t_p} dt \frac{dR}{dt}(t, t_n) R^2(t, t_n) \epsilon(t)$$

- $\epsilon(t)$: latent heat ($\sim$ vacuum energy)
- κ_ν: fraction of energy going into the wall motion (vs. heating the plasma)

$\bar{R}$ and E_{kin}: key parameters to deduce the GW spectrum

Some assumptions

Entire dynamics specified by $\Gamma(t)$, $\epsilon(t)$, κ_ν, $v(t)$ and $a(t)$.

Some assumptions

Entire dynamics specified by $\Gamma(t)$, $\epsilon(t)$, κ_ν, $v(t)$ and $a(t)$.

Very strong PT:

- large amount of vacuum energy released
- $\Rightarrow \kappa_\nu \sim 1$ [A. Kobakhidze et al, arXiv:1607.00883]
- $\Rightarrow v \sim 1$ (runaway bubbles) [C. Caprini et al., JCAP 1604 (2016) no.04 001]

Some assumptions

Entire dynamics specified by $\Gamma(t)$, $\epsilon(t)$, κ_ν, $v(t)$ and $a(t)$.

Very strong PT:

- large amount of vacuum energy released
- $\Rightarrow \kappa_\nu \sim 1$ [A. Kobakhidze et al, arXiv:1607.00883]
- $\Rightarrow v \sim 1$ (runaway bubbles) [C. Caprini et al., JCAP 1604 (2016) no.04 001]

Consider a radiation-dominated Universe:

- $a(t) \propto t^{1/2}$
- $t = \left(\frac{45M_p^2}{16\pi^3 g_\star}\right)^{1/2} \frac{1}{T^2}$
- need to confirm this assumption at low temperature (see below)

Numerical results

Probability $p(T)$:

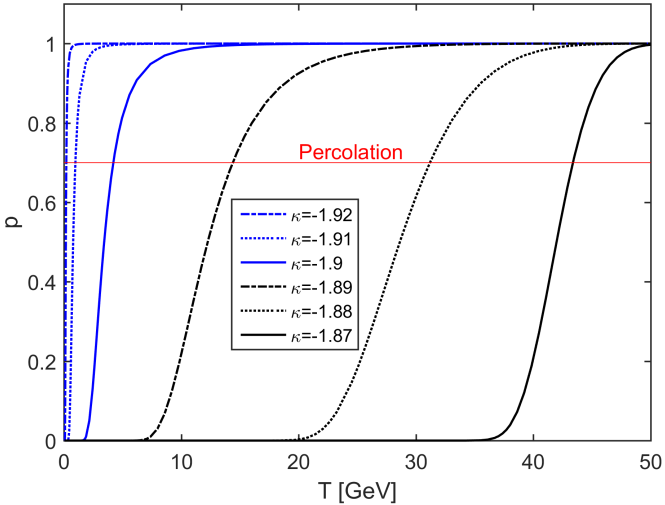

Number density distribution for $|\bar{\kappa}| = 1.9$: $\Rightarrow T_n \sim 49$ GeV

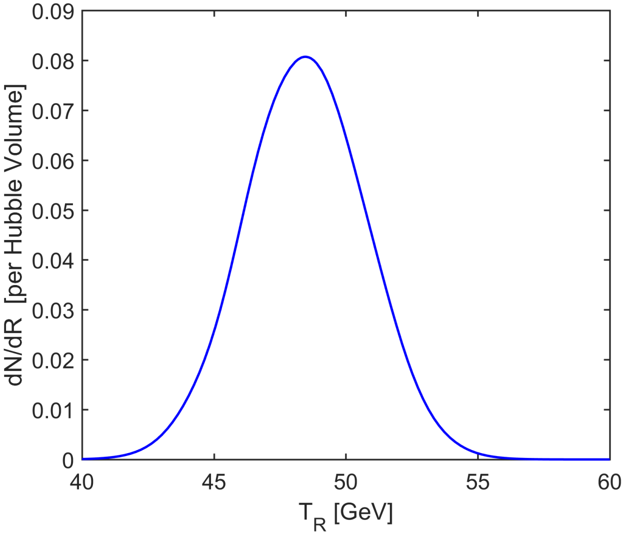

Numerical results

$\kappa\ [m_h^2/\lvert v\rvert]$	$T_\star$ GeV	T_n GeV	T_p GeV	$(\bar{R}H_p)^{-1}$	$\rho_{\text{kin}}/\rho_{\text{rad}}$
-1.87	85.9	48.9	43.4	8.79	0.57
-1.88	85.5	48.9	31.2	2.76	1.88
-1.89	84.5	49.0	14.4	1.41	37.8
-1.9	84.1	48.7	4.21	1.09	$5.09 \cdot 10^3$
-1.91	83.9	48.6	0.977	1.02	$1.73 \cdot 10^6$
-1.92	83.3	48.5	0.205	1.00	$8.80 \cdot 10^8$

Observations:

- new feature: $T_p \ll T_n$
- Hubble-size bubbles at collision
- $\rho_{\text{rad}} \ll \rho_{\text{kin}}$: confirm very strong scenario

Discussing the equation of state

$T \searrow \Rightarrow \rho_{\text{rad}} \propto T^4 \searrow \Rightarrow$ vacuum energy might dominate: small-field inflation?

Discussing the equation of state

$T \searrow \Rightarrow \rho_{\text{rad}} \propto T^4 \searrow \Rightarrow$ vacuum energy might dominate: small-field inflation?

Two scenarios:

- $T_p \sim T_n \ll T_{EW}$: inflation indeed occurs [T. Konstandin and G. Servant, JCAP 1112 (2011) 009]
- $T_p \ll T_n \lesssim T_{EW}$: bubbles produced before vacuum-radiation equality

  $\Rightarrow$ vacuum energy transferred to bubble-walls $+$ inhomogeneous Universe

  $\Rightarrow$ very likely to prevent small-field inflation

[Brandenberger, Int.J.Mod.Phys. D26 (2016) no.01, 1740002]

Discussing the equation of state

$T \searrow \Rightarrow \rho_{\text{rad}} \propto T^4 \searrow \Rightarrow$ vacuum energy might dominate: small-field inflation?

Two scenarios:

- $T_p \sim T_n \ll T_{EW}$: inflation indeed occurs [T. Konstandin and G. Servant, JCAP 1112 (2011) 009]
- $T_p \ll T_n \lesssim T_{EW}$: bubbles produced before vacuum-radiation equality

  $\Rightarrow$ vacuum energy transferred to bubble-walls + inhomogeneous Universe

  $\Rightarrow$ very likely to prevent small-field inflation

[Brandenberger, Int.J.Mod.Phys. D26 (2016) no.01, 1740002]

For example $|\bar{\kappa}| = 1.9$:

- vacuum-radiation equality at $(T \sim 36$ GeV $) < (T_n \sim 49$ GeV$)$
- inhomogeneity at $T \sim 36$ GeV: 0.47 bubbles per Hubble volume with size 26% of Hubble radius

Gravitational wave signal

GWs from bubble collisions

Stochastic background from three sources [C. Caprini et al., JCAP 1604 (2016) no.04 001]:

$$h^2\Omega_{\mathrm{GW}}(f) \simeq h^2\Omega_{col} + h^2\Omega_{sw} + h^2\Omega_{\mathrm{MHD}}$$

GWs from bubble collisions

Stochastic background from three sources [C. Caprini et al., JCAP 1604 (2016) no.04 001]:

$$h^2\Omega_{\mathrm{GW}}(f) \simeq h^2\Omega_{col} + h^2\Omega_{sw} + h^2\Omega_{\mathrm{MHD}}$$

Ω_{col} dominant for very strong PT

GWs from bubble collisions

Stochastic background from three sources [C. Caprini et al., JCAP 1604 (2016) no.04 001]:

$$h^2\Omega_{\mathsf{GW}}(f) \simeq h^2\Omega_{col} + h^2\Omega_{sw} + h^2\Omega_{\mathsf{MHD}}$$

Ω_{col} dominant for very strong PT

Dimensional analysis:

- peak frequency from collision: $f_{\mathsf{peak}}(t_p) \sim (\bar{R})^{-1}$
- peak amplitude at collision: $\Omega_{col}(f_p) \sim (\bar{R}H_p)^2 \frac{\rho_{\mathsf{kin}}^2}{(\rho_{\mathsf{kin}}+\rho_{\mathsf{rad}})^2}$

GWs from bubble collisions

Stochastic background from three sources [C. Caprini et al., JCAP 1604 (2016) no.04 001]:

$$h^2\Omega_{\mathrm{GW}}(f) \simeq h^2\Omega_{col} + h^2\Omega_{sw} + h^2\Omega_{\mathrm{MHD}}$$

Ω_{col} dominant for very strong PT

Dimensional analysis:

- peak frequency from collision: $f_{\mathrm{peak}}(t_p) \sim (\bar{R})^{-1}$
- peak amplitude at collision: $\Omega_{col}(f_p) \sim (\bar{R}H_p)^2 \frac{\rho_{\mathrm{kin}}^2}{(\rho_{\mathrm{kin}}+\rho_{\mathrm{rad}})^2}$

Then redshift from collision time to today

Bubble-collision simulations

Going beyond dimensional analysis with state-of-the-art numerical simulations (and redshift) [S. Huber and T. Konstandin, JCAP 0809 (2008) 022]

Bubble-collision simulations

Going beyond dimensional analysis with state-of-the-art numerical simulations (and redshift) [S. Huber and T. Konstandin, JCAP 0809 (2008) 022]

Notation: $\alpha = \rho_{\mathsf{kin}}/\rho_{\mathsf{rad}}$ and $\beta = v\bar{R}^{-1} \sim \bar{R}^{-1}$

Bubble-collision simulations

Going beyond dimensional analysis with state-of-the-art numerical simulations (and redshift) [S. Huber and T. Konstandin, JCAP 0809 (2008) 022]

Notation: $\alpha = \rho_{\mathrm{kin}}/\rho_{\mathrm{rad}}$ and $\beta = v\bar{R}^{-1} \sim \bar{R}^{-1}$

Amplitude:

$$h^2\Omega_{col}(f) = 1.67 \times 10^{-5} \left(\frac{100}{g_*}\right)^{1/3} \left(\frac{\beta}{H_p}\right)^{-2} \kappa_v^2 \left(\frac{\alpha}{1+\alpha}\right)^2 \left(\frac{0.11 v^3}{0.42 + v^2}\right) S(f)$$

$$S(f) = \frac{3.8 (f/f_0)^{2.8}}{1 + 2.8 (f/f_0)^{3.8}}$$

Bubble-collision simulations

Going beyond dimensional analysis with state-of-the-art numerical simulations (and redshift) [S. Huber and T. Konstandin, JCAP 0809 (2008) 022]

Notation: $\alpha = \rho_{\text{kin}}/\rho_{\text{rad}}$ and $\beta = v\bar{R}^{-1} \sim \bar{R}^{-1}$

Amplitude:

$$h^2\Omega_{col}(f) = 1.67 \times 10^{-5} \left(\frac{100}{g_*}\right)^{1/3} \left(\frac{\beta}{H_p}\right)^{-2} \kappa_v^2 \left(\frac{\alpha}{1+\alpha}\right)^2 \left(\frac{0.11v^3}{0.42+v^2}\right) S(f)$$

$$S(f) = \frac{3.8(f/f_0)^{2.8}}{1+2.8(f/f_0)^{3.8}}$$

Peak frequency:

$$f_0 = 1.65 \times 10^{-7} \left(\frac{T_p}{1\text{ GeV}}\right) \left(\frac{g_*}{100}\right)^{1/6} H_p^{-1} \beta \left(\frac{0.62}{1.8 - 0.1v + v^2}\right) \text{Hz}$$

Bubble-collision simulations

Going beyond dimensional analysis with state-of-the-art numerical simulations (and redshift) [S. Huber and T. Konstandin, JCAP 0809 (2008) 022]

Notation: $\alpha = \rho_{\text{kin}}/\rho_{\text{rad}}$ and $\beta = v\bar{R}^{-1} \sim \bar{R}^{-1}$

Amplitude:

$$h^2\Omega_{col}(f) = 1.67 \times 10^{-5} \left(\frac{100}{g_*}\right)^{1/3} \left(\frac{\beta}{H_p}\right)^{-2} \kappa_v^2 \left(\frac{\alpha}{1+\alpha}\right)^2 \left(\frac{0.11 v^3}{0.42 + v^2}\right) S(f)$$

$$S(f) = \frac{3.8 (f/f_0)^{2.8}}{1 + 2.8 (f/f_0)^{3.8}}$$

Peak frequency:

$$f_0 = 1.65 \times 10^{-7} \left(\frac{T_p}{1 \text{ GeV}}\right) \left(\frac{g_*}{100}\right)^{1/6} H_p^{-1} \beta \left(\frac{0.62}{1.8 - 0.1 v + v^2}\right) \text{Hz}$$

To discuss further: applicability of these simulations to large bubbles ($\sim$long-lasting PT)

GW spectra: results

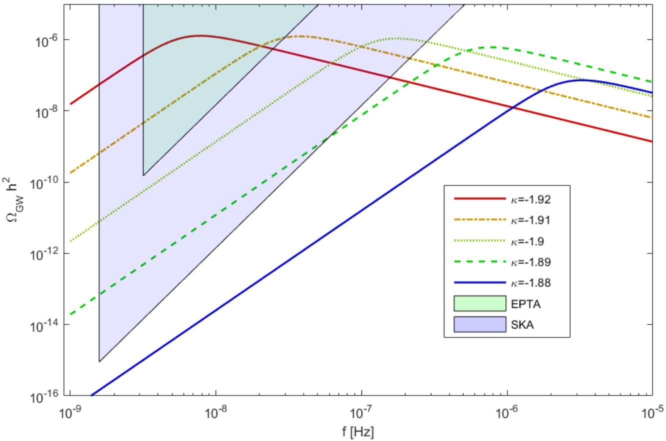

- Current constraints: EPTA, PPTA, NANOGrav
- Possible detection: Square Kilometre Array

[Moore et al., Class. Quant. Grav. 32 (2015) 015014]

Summary of Part II

- Study of a very strong and prolonged EWPT:

$$T_n \sim 50 \text{ GeV and } T_p \sim [0.2 - 10] \text{ GeV}$$

Summary of Part II

- Study of a very strong and prolonged EWPT:

$$T_n \sim 50 \text{ GeV and } T_p \sim [0.2 - 10] \text{ GeV}$$

- Stochastic GWs detectable by PTA detectors:

new way of probing EWPT!

Summary of Part II

- Study of a very strong and prolonged EWPT:

$$T_n \sim 50 \text{ GeV} \text{ and } T_p \sim [0.2 - 10] \text{ GeV}$$

- Stochastic GWs detectable by PTA detectors:

new way of probing EWPT!

- Open questions:

exact equation of state and validity of GW fitting formula

Summary of Part II

- Study of a very strong and prolonged EWPT:

  $T_n \sim 50$ GeV and $T_p \sim [0.2 - 10]$ GeV

- Stochastic GWs detectable by PTA detectors:

  new way of probing EWPT!

- Open questions:

  exact equation of state and validity of GW fitting formula

- Not limited to the model discussed here (just need a barrier at T=0):

  e.g. singlet extensions of SM or NMSSM

General Conclusion

- The detection of Gravitational Waves represents a milestone by itself.

General Conclusion

- The detection of Gravitational Waves represents a milestone by itself.

- It also provides new opportunities to probe various area of fundamental physics from General Relativity to Particle Physics.

General Conclusion

- The detection of Gravitational Waves represents a milestone by itself.
- It also provides new opportunities to probe various area of fundamental physics from General Relativity to Particle Physics.
- There are lot of expectations regarding the future experiments like KAGRA, LISA, SKA, etc